Supplementary Information

This supplementary information contains:

Supplementary Table 1: Antibodies used in this study

Supplementary Dataset 1: Sequence data from analysis of plasmablasts from PfSPZ vaccinated volunteers

Supplementary Figures 1-6

Supplementary Table 1: Antibodies used in this study

A. Anti-mouse antibodies for flow cytometry and magnetic column sorting

Antigen	Conjugate	Clone	Source	Catalogue	Concentration	Dilution
Anti-mouse B220	APC	RA3-6B2	Biolegend	103212	0.2 mg/mL	1/400
Anti-mouse B220	BV605	RA3-6B2	BioLegend	103244	0.2 mg/mL	1/400
Anti-mouse B220	PE-Cy7	RA3-6B2	BD Pharmigen	552772	0.2mg/mL	1/200
Anti-mouse CD3	PerCP Cy5.5	17A2	Biolegend	100218	0.2 mg/mL	1/200
Anti-mouse CD4	APC	RM4-5	Biolegend	100516	0.2 mg/mL	1/200
Anti-mouse CD4	Biotin	GK1.5	Biolegend	100404	0.5 mg/mL	1/200
Anti-mouse CD5	APC	537.3	eBioscience	17-0051-82	0.2mg/mL	1/400
Anti-mouse CD8a	Biotin	53-6.7	Biolegend	100704	0.5 mg/mL	1/200
Anti-mouse CD8a	BV421	53-6.7	Biolegend	100738	0.2 mg/mL	1/200
Anti-mouse CD8a	FITC	5H10-1	Biolegend	100804	0.5 mg/mL	1/200
Anti-mouse CD11a	PE Cy7	M17/4	Biolegend	101122	0.2 mg/mL	1/200
Anti-mouse CD11b	FITC	M1/70	Biolegend	101206	0.5 mg/mL	1/100
Anti-mouse CD11b	PerCP Cy5.5	M1/70	Biolegend	101228	0.2 mg/mL	1/200
Anti-mouse CD11c	PerCP Cy5.5	N418	Biolegend	117328	0.2 mg/mL	1/200
Anti-mouse CD19	BUV395	1D3	BD Horizon	563557	0.2 mg/mL	1/200
Anti-mouse CD21/35	FITC	7G6	BD Pharmigen	553818	0.5mg/ml	1/400
Anti-mouse CD23	Pac Blue	B3B4	Biolegend	101616	0.5mg/ml	1/200
Anti-mouse CD24	Pac Blue	M1/69	Biolegend	101820	0.5 mg/mL	1/200
Anti-mouse CD28	APC	E18	Biolegend	122016	0.2mg/mL	1/200
Anti-mouse CD38	A700	90	eBioscience	56-0381-82	0.2 mg/mL	1/200
Anti-mouse CD43	BB515	57	BD Horizon	564646	0.2mg/mL	1/200
Anti-mouse CD44	Pac Blue	IM7	Biolegend	103020	0.5mg/ml	1/400
Anti-mouse CD45.1	BV510	A20	Biolegend	110741	0.2mg/ml	1/200

Anti-mouse CD45.1	FITC	A20	Biolegend	110706	0.5 mg/mL	1/200
Anti-mouse CD45.1	PE	A20	Biolegend	110708	0.2mg/mL	1/200
Anti-mouse CD45.2	FITC	104	Invitrogen	11-0454-82	0.5 mg/mL	1/200
Anti-mouse CD45.2	PE	104	Biolegend	109807	0.2 mg/mL	1/200
Anti-mouse CD80	BV421	16-10A1	Biolegend	104725	0.2mg/mL	1/400
Anti-mouse CD80	PE CY7	16-10A1	Biolegend	104734	0.2 mg/mL	1/200
Anti-mouse CD93	APC	AA4.1	eBioscience	17-5892-82	0.2 mg/mL	1/100
Anti-mouse CD138	Biotin	281-2	Biolegend	142512	0.5 mg/mL	1/200
Anti-mouse CD138	BV510	281-2	Biolegend	142521	0.2 mg/mL	1/300
Anti-mouse CD138	PE Cy7	281-2	Biolegend	142514	0.2 mg/mL	1/300
Anti-mouse CD273 (PDL2)	APC	TY25	Biolegend	107210	0.2 mg/mL	1/200
Anti-mouse GL7	A.488	GL7	Biolegend	144612	0.5 mg/mL	1/400
Anti-mouse GL7	Biotin	GL7	Biolegend	144616	0.5 mg/mL	1/200
Anti-mouse GL7	eFluor450	GL-7	Invitrogen	48-5902-82	0.2 mg/mL	1/100
Anti-mouse IgD	BV605	11-26c.2a	Biolegend	405727	0.2 mg/mL	1/400
Anti-mouse IgM	APC-eFluor780	II/41	Invitrogen	47-5790-82	0.2 mg/mL	1/200
Anti-mouse Ly-6G/Ly-6C (GR1)	PerCP Cy5.5	RB6-8C5	Biolegend	108428	0.2 mg/mL	1/200
Anti-mouse NK1.1	PE-CY7	PK136	Biolegend	108714	0.2mg/mL	1/200
TruStain fcX (rat anti-mouse CD16/32):	-	93	Biolegend	101320	0.5 mg/mL	1/50
7AAD Cell Viability Dye	PerCP Cy5.5	-	Biolegend	420404	50 µg/mL	1/100

B. Anti-human antibodies for flow cytometry

Antigen	Conjugate	Clone	Source	Catalogue
Anti-human CD19	FITC	HIB19	BD Bioscience	555412
Anti-human CD20	APC-Cy7	L27	BD Bioscience	335794
Anti-human CD27	APC	O323	ThermoFisher	17-0279-42

Anti-human CD3	PE-Cy7	SK7	BD Bioscience	557851
Anti-human CD38	PE	HIT	BD Bioscience	555460
Live Dead Aqua	-	-	Invitrogen	L34966

C. Antibodies for ELISA and ELIspot

Antigen	Conjugate	Source	Catalogue	Concentration	Dilution
Anti-human IgG (H+L) - produced in goat	HRP	Seracare	5220-0330	1mg/ml	1/2000
Anti-mouse IgG (H+L) - produced in goat	HRP	Seracare	5220-0341	1mg/ml	1/2000
Anti-mouse IgM (μ) - produced in goat	HRP	Seracare	074-1803	1mg/ml	1/2000

Supplementary Dataset 1: Sequence data from analysis of plasmablasts from PfSPZ vaccinated volunteers. Complete details of sequences and specificities for all plasmablasts isolated from vaccinated donors. CSP reactive cells are denoted in grey if the sole representative of a clone. Individual members of expanded clones are colour coded according to the clone they belong to.

Supplementary Figure Legends

Supplementary Figure 1: Isolation and screening of human plasmablasts.

PfSPZ vaccinated individuals were bled one week after each boost and plasmablasts sorted, their BCR genes were cloned and expressed and measured for reactivity with CSP by ELISA or electrochemiluminescence. A. Gating strategy for the single cell sorting of human plasmablasts. B. CSP reactivity of each antibody cloned from the plasmablasts at the different time. CSP reactivity was measured by ELISA (615 all timepoints; 606 V2) or electrochemiluminescence (608 all timepoints; 606 V1 and V3). For both techniques background cut-off for CSP reactivity was set at Median +4MAD. Data are expressed as % of maximum value with the background subtracted.

Supplementary Figure 2: Generation and phenotyping of the Igh^{g2A10} mouse.

A. Schematic of the insertion of the rearranged heavy chain VDJ exon upstream of the IgM locus. B. Gating strategy for phenotyping of splenic B cell subsets (i) and relative percentages of splenic lymphocyte subsets in Igh^{g2A10} mice compared with C57BL/6 mice (ii). C. Gating strategy for B cell subsets within bone marrow (i) and relative percentages (ii). D. Gating strategy for B cell subsets within peritoneal cavity (i) and relative percentages (ii). G. Strategy for identification of Igh^{g2A10} B cells following adoptive transfer to congenic recipient mice. H. Strategy for identification of tetramer^{+} Igh^{g2A10} long lived plasma cells in the bone marrow of recipient mice when using congenic markers to sort cells (i) or using Igh^{g2A10} *Blimp*$^{GFP/+}$ reporter cells (ii). All analyses between the Igh^{g2A10} and C57BL/6 performed using a Student's t-test for each pairwise comparison; means ± s.d shown.

Supplementary Figure 3: CSP-reactive Igh^{g2A10} cells undergo affinity maturation.

Single tetramer^{+} Igh^{2A10} BMPCs were sorted from mice 1 month after transfer of 2 x10^{4} Igh^{g2A10} cells and vaccination with 5 x 10^{4} Pb-PfCSP SPZ and the BCR sequenced. The locations of mutations in the heavy chain (A) and light chain (B) are shown for IgG^{+} and IgM^{+} plasmablasts and compared to the sites of mutations in the 2A10 monoclonal antibody. Mutations that are annotated at the top of each are those that have been previously validated as increasing affinity over the germline unmutated precursor.

Supplementary Figure 4: Isolation and phenotyping of PfCSP-specific memory B cells.

A. Phenotype of memory B cells generated 2 months after transfer 2 x10^{4} Igh^{g2A10} cells and immunization with either 5 x 10^{4} Pb-PfCSP SPZ or 30 μg PfCSP in Alum. Fluorescence-minus-one (FMO) staining controls for CD80 and PDL2 also shown. B. Relative percentage of PDL2^{+} and CD80^{+} memory cell subsets generated from either immunogen. C. Memory B cells prepared as in A. were depleted of T cells, GC B cells and Plasmablasts and analysed to confirm the efficiency of enrichment. Panels show the Igh^{g2A10} B cells populations present in the immunised recipients with and without the depletion of non-memory B cell using magnetic columns. Once memory Igh^{g2A10} cell suspensions were depleted of other contaminating B cell populations they were then used for adoptive transfer to naïve or immune recipients.

Supplementary Figure 5: Delayed boosting allows enhanced recall responses.

A. Schematic of the vaccination schedule for the experiment. B. Concentration of IgG anti-$(NANP)_9$ antibodies in the sera of mice immunized as in A; each icon denotes an individual serum sample with bars showing means ± sd. C. Representative flow cytometry plots for the identification of Igh^{g2A10} B populations within the spleens of recipient mice. Summary data for the analysis of spleen PBs (D), spleen GC B cells (E), spleen memory B cells (F) and BMPCs (G) at the indicated timepoints; data are pooled from 2 replicate experiments, analysis was by one-way ANOVA including the experiment as a blocking factor, bars show means ± s.d..

Supplementary Figure 6: Binding of repeat and non-repeat specific monoclonal antibodies to PfCSP by bilayer interferometry.

Avidity of 2A10, 5D5 and mAb15 antibodies for rPfCSP. Antibody binding curves are shown in black (raw data). Data were fitted (dotted red lines) with the binding equations describing a 1:1 heterologous ligand interaction. Serial concentrations of antibodies used are as denoted to the right of each graph (n = 3, representative experiment is shown). Table shows the inferred binding kinetics of each antibody for PfCSP and associated errors.

Supplementary Figure 1

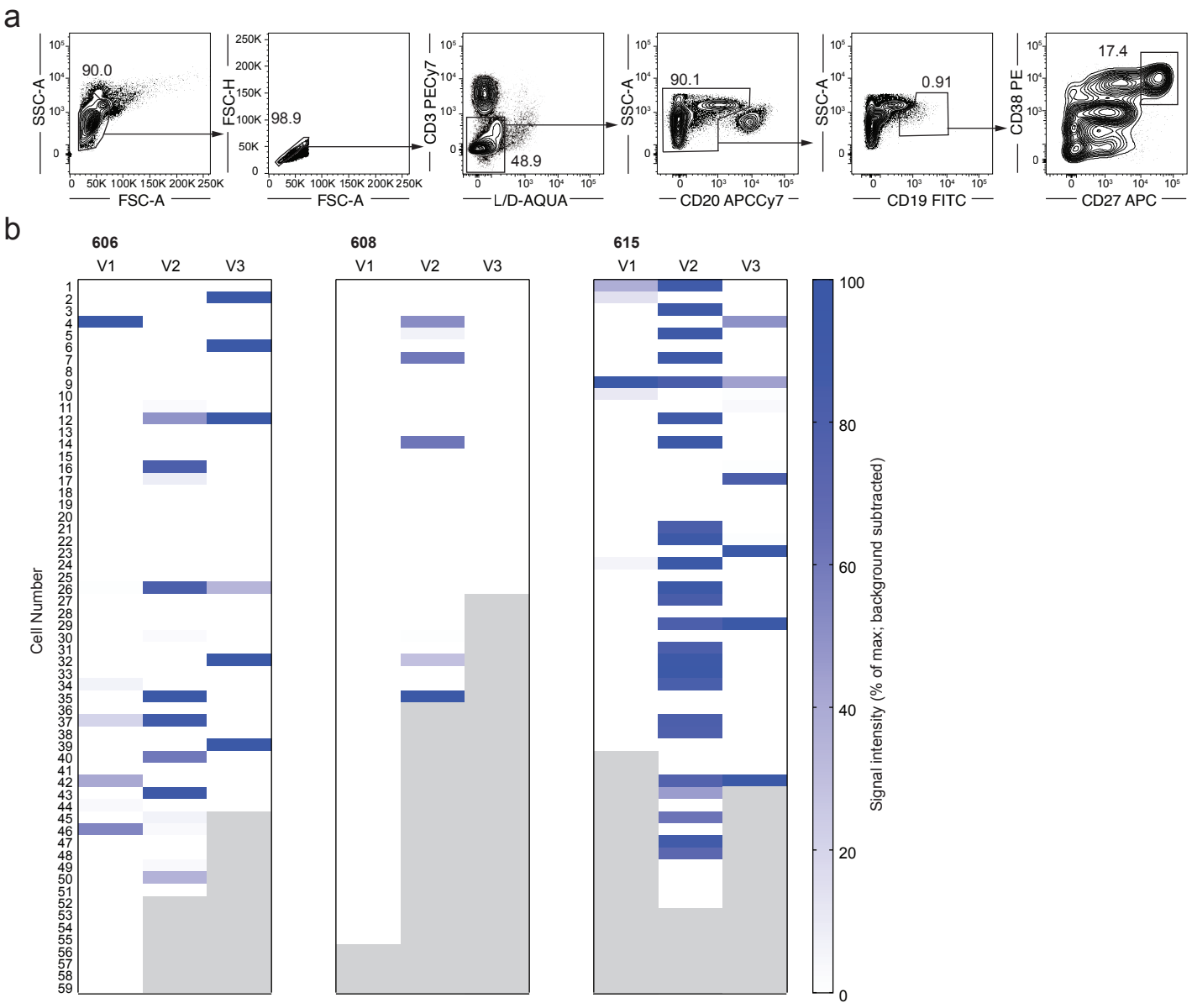

Supplementary Figure 1: Isolation and screening of human plasmablasts.
PfSPZ vaccinated individuals were bled one week after each boost and plasmablasts sorted, their BCR genes were cloned and expressed and measured for reactivity with CSP by ELISA or electrochemiluminescence. A. Gating strategy for the single cell sorting of human plasmablasts. B. CSP reactivity of each antibody cloned from the plasmablasts at the different time. CSP reactivity was measured by ELISA (615 all timepoints; 606 V2) or electrochemiluminescence (608 all timepoints; 606 V1 and V3). For both techniques background cut-off for CSP reactivity was set at Median +4MAD. Data are expressed as % of maximum value with the background subtracted.

Supplementary Figure 2

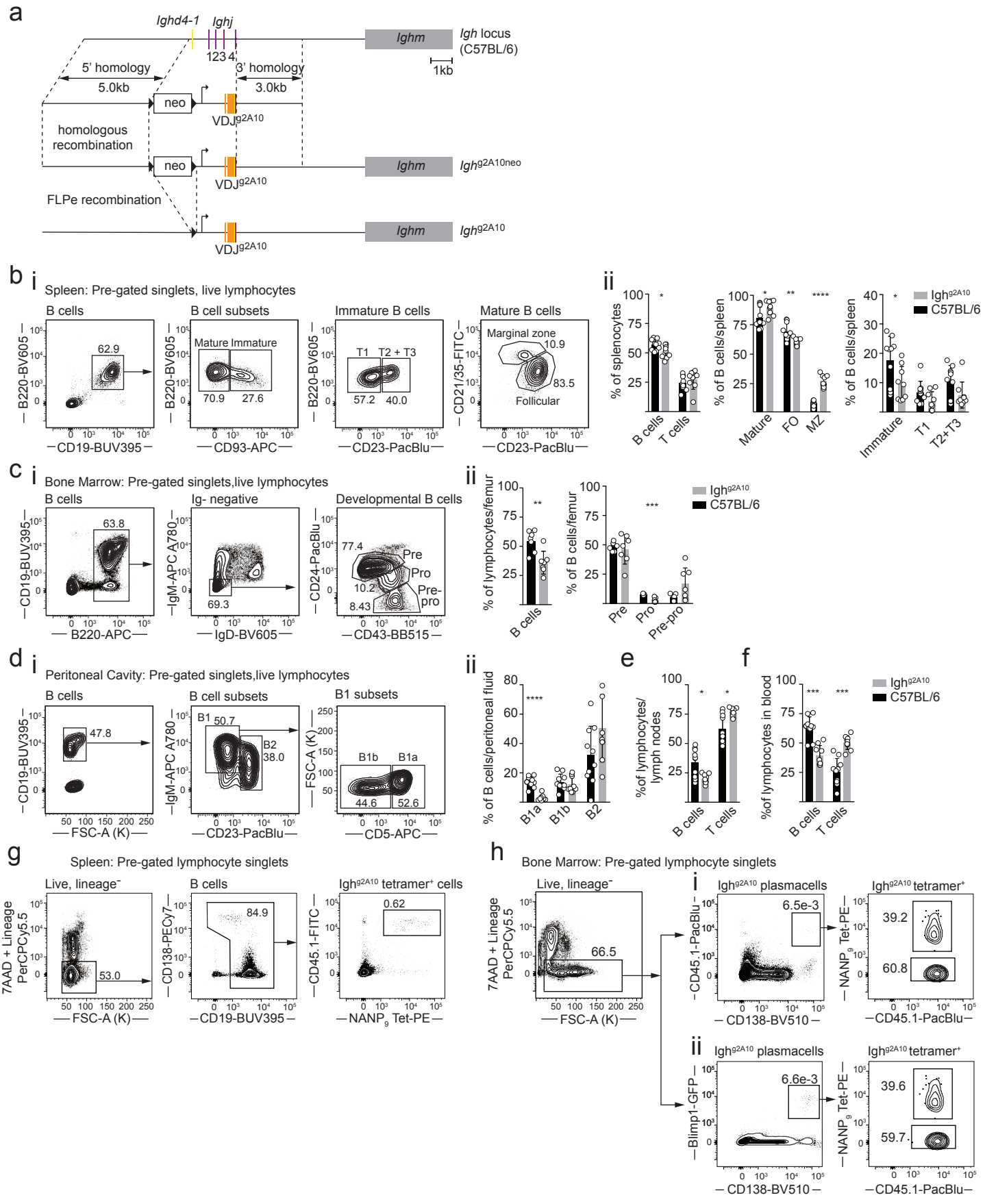

Supplementary Figure 2: Generation and phenotyping of the Igh^{g2A10} mouse.
A. Schematic of the insertion of the rearranged heavy chain VDJ exon upstream of the IgM locus. B. Gating strategy for phenotyping of splenic B cell subsets (i) and relative percentages of splenic lymphocyte subsets in Igh^{g2A10} mice compared with C57BL/6 mice (ii). C. Gating strategy for B cell subsets within bone marrow (i) and relative percentages (ii). D. Gating strategy for B cell subsets within peritoneal cavity (i) and relative percentages (ii). G. Strategy for identification of Igh^{g2A10} B cells following adoptive transfer to congenic recipient mice. H. Strategy for identification of tetramer+ Igh^{g2A10} long lived plasma cells in the bone marrow of recipient mice when using congenic markers to sort cells (i) or using Ighg2A10 BlimpGFP/+ reporter cells (ii). All analyses between the Igh^{g2A10} and C57BL/6 performed using a Student's t-test for each pairwise comparison; means s.d shown.

Supplementary Figure 3

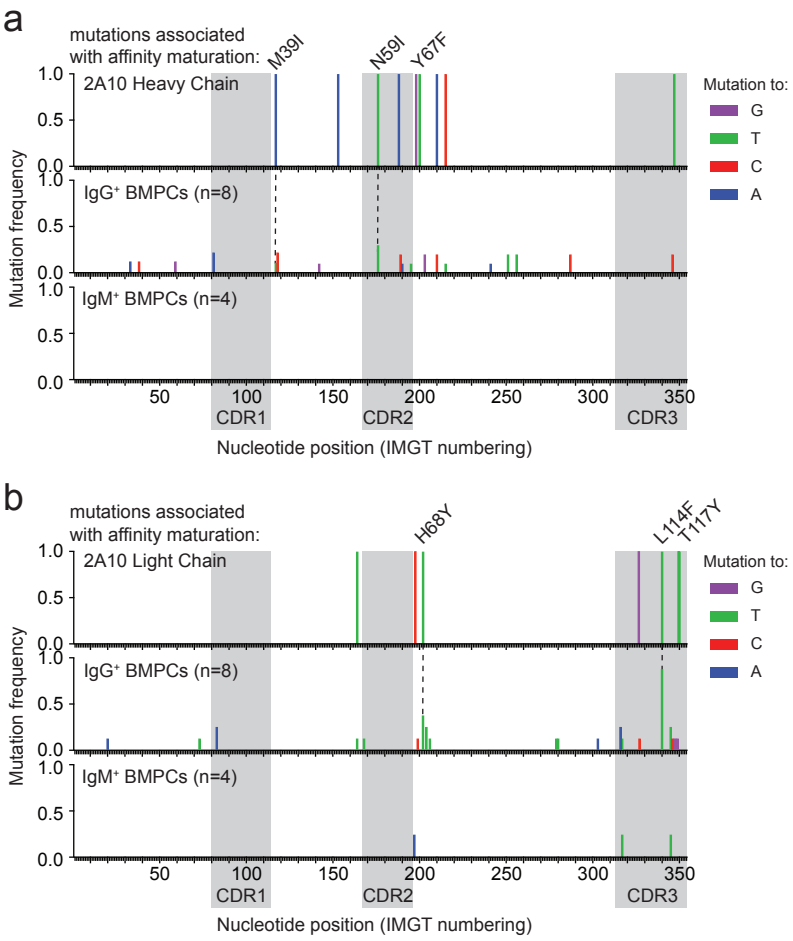

Supplementary Figure 3: CSP-reactive Igh^{g2A10} cells undergo affinity maturation.
Single tetramer+ Ig^{h2A10} BMPCs were sorted from mice 1 month after transfer of 2 x10^4 Igh^{g2A10} cells and vaccination with 5 x 104 Pb-PfCSP SPZ and the BCR sequenced. The locations of mutations in the heavy chain (A) and light chain (B) are shown for IgG+ and IgM+ plasmablasts and compared to the sites of mutations in the 2A10 monoclonal antibody. Mutations that are annotated at the top of each are those that have been previously validated as increasing affinity over the germline unmutated precursor.

Supplementary Figure 4

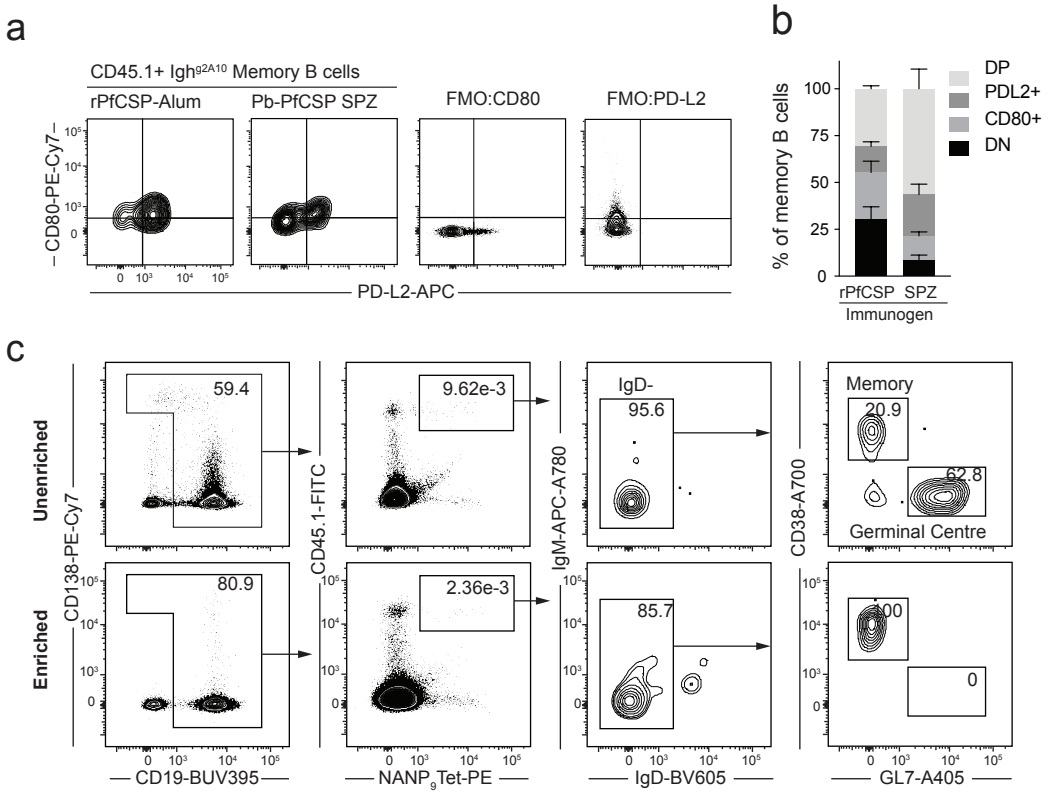

Supplementary Figure 4: Isolation and phenotyping of PfCSP-specific memory B cells
A. Phenotype of memory B cells generated 2 months after transfer 2 x104 Igh^{g2A10} cells and immunization with either 5 x 104 Pb-PfCSP SPZ or 30 g PfCSP in Alum. Fluorescence-minus-one (FMO) staining controls for CD80 and PDL2 also shown. B. Relative percentage of PDL2+ and CD80+ memory cell subsets generated from either immunogen. C. Memory B cells prepared as in A. were depleted of T cells, GC B cells and Plasmablasts and analysed to confirm the efficiency of enrichment. Panels show the Igh^{g2A10} B cells populations present in the immunised recipients with and without the depletion of non-memory B cell using magnetic columns. Once memory Igh^{g2A10} cell suspensions were depleted of other contaminating B cell populations they were then used for adoptive transfer to naïve or immune recipients.

Supplementary Figure 5

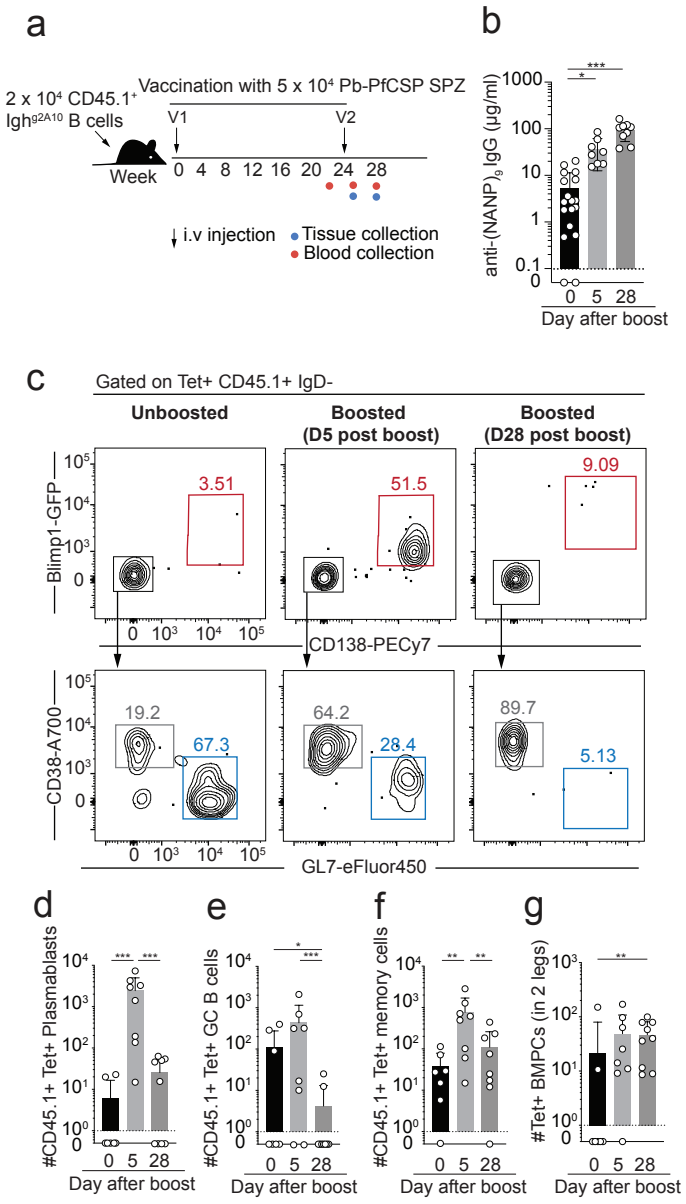

Supplementary Figure 5: Delayed boosting allows enhanced recall responses.
A. Schematic of the vaccination schedule for the experiment. B. Concentration of IgG anti-$(NANP)_9$ antibodies in the sera of mice immunized as in A; each icon denotes an individual serum sample with bars showing means sd. C. Representative flow cytometry plots for the identification of Igh^{g2A10} B populations within the spleens of recipient mice. Summary data for the analysis of spleen PBs (D), spleen GC B cells (E), spleen memory B cells (F) and BMPCs (G) at the indicated timepoints; data are pooled from 2 replicate experiments, analysis was by one-way ANOVA including the experiment as a blocking factor, bars show means s.d..

Supplementary Figure 6

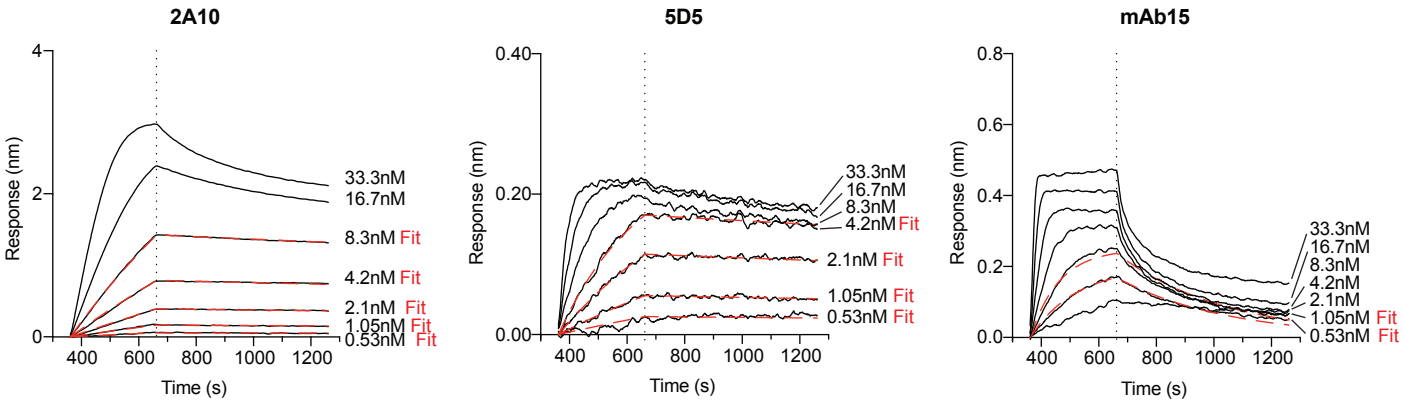

mAb ID	K_D (M)	K_D Error	k_{on}(1/Ms)	k_{on} Error	k_{dis}(1/s)	k_{dis} Error
2A10	$1.05x10^{-9}$	$4.08x10^{-11}$	$1.20x10^{5}$	$3.98x10^{3}$	$1.27x10^{4}$	$2.55x10^{6}$
5D5	$1.76x10^{-10}$	$1.43x10^{-11}$	$7.91x10^{5}$	$3.36x10^{4}$	$1.39x10^{4}$	$9.67x10^{6}$
mAb15	$7.42x10^{-10}$	$4.47x10^{-11}$	$3.54x10^{6}$	$2.06x10^{5}$	$2.62x10^{3}$	$4.18x10^{5}$

Supplementary Figure 6: Binding of repeat and non-repeat specific monoclonal antibodies to PfCSP by bilayer interferometry

Avidity of 2A10, 5D5 and mAb15 antibodies for rPfCSP. Antibody binding curves are shown in black (raw data). Data were fitted (dotted red lines) with the binding equations describing a 1:1 heterologous ligand interaction. Serial concentrations of antibodies used are as denoted to the right of each graph (n = 3, representative experiment is shown). Table shows the inferred binding kinetics of each antibody for PfCSP and associated errors.